

## Supplementary Material for:

### “A Dataset Generation Framework for Symmetry-Induced Mechanical Metamaterials”

#### 1. Samples and Possible Representations

In this document, we introduce some samples generated from the proposed method of utilizing material crystallographic symmetries in the establishment of truss material. It is important to note that this dataset is not yet complete and cannot be utilized to train a machine learning model at the current stage. The main idea of this section is to demonstrate how data generated from the proposed method can be represented in various formats. The samples used in generating the data in this paper can be found in the following documents:

<https://github.com/DreamLabUIC/Symmetry-Induced-Mechanical-Metamaterials>

Each line in the files attached to the link represents the entire dataset related to a specific topology. We have included all of them in the same file to simplify the illustration. All the stiffness components were obtained for a solid base material with a Young’s modulus ( $E_s$ ) of 200 GPa, a Poisson’s ratio ( $\nu$ ) of 0.3, and a truss diameter of 0.025 m. The dataset generation method provided allows for the creation of data that can be represented in multiple formats, such as parametric and graph representations. These representations illustrate the versatility and depth of truss-based metamaterials design. They enable clear visualization of the symmetrical properties and potential applications by using these representations in machine learning applications, providing a fundamental tool for advancing research in mechanical metamaterial science.

Supp. Table 1. Graph representation of a cubic sample.

Data representation in the file															
0.296002 0.197849 0.197849 -0.000000 0.000000 0.000000 0.296002 0.197849 -0.000000 0.000000 0.000000 0.296002 0.000000 -0.000000 -0.000000 0.114547 -0.000000 -0.000000 0.114547 0.000000 0.114547 0.500000 0.500000 0.500000 0.500000 0.333333 0.333333 0.333333 0.333333 0.333333 v <sub>0</sub> f <sub>1</sub> e <sub>4</sub>															
Effective Elastic Properties (Stiffness Components)															
0.296002 0.197849 0.197849 -0.000000 0.000000 0.000000 0.296002 0.197849 -0.000000 0.000000 0.000000 0.296002 0.000000 -0.000000 -0.000000 0.114547 -0.000000 -0.000000 0.114547 0.000000 0.114547															
Topological representation pre – reflection															
$C = \begin{bmatrix} 0.500 & & & & & & & \\ & \vdots \\ & v_0 & v_1 & v_2 & v_3 & e_0 & e_1 & e_2 & e_3 & e_4 & e_5 & f_0 & f_1 & f_2 & f_3 \\ & 0 & 1 & 0 & 0 & 0 & 0 & 0 & 0 & 0 & 0 & 0 & 1 & 0 & 0 & 0 \\ & v_1 & 0 & 1 & 0 & 0 & 0 & 0 & 0 & 0 & 0 & 0 & 0 & 0 & 0 & 0 & 0 \\ & v_2 & 0 & 0 & 1 & 0 & 0 & 0 & 0 & 0 & 0 & 0 & 0 & 0 & 0 & 0 & 0 \\ & v_3 & 0 & 0 & 0 & 1 & 0 & 0 & 0 & 0 & 0 & 0 & 0 & 0 & 0 & 0 & 0 \\ & e_0 & 0 & 0 & 0 & 0 & 1 & 0 & 0 & 0 & 0 & 0 & 0 & 0 & 0 & 0 & 0 \\ & e_1 & 0 & 0 & 0 & 0 & 0 & 1 & 0 & 0 & 0 & 0 & 0 & 0 & 0 & 0 & 0 \\ & e_2 & 0 & 0 & 0 & 0 & 0 & 0 & 1 & 0 & 0 & 0 & 0 & 0 & 0 & 0 & 0 \\ & e_3 & 0 & 0 & 0 & 0 & 0 & 0 & 0 & 1 & 0 & 0 & 0 & 1 & 0 & 0 & 0 \\ & e_4 & 0 & 0 & 0 & 0 & 0 & 0 & 0 & 0 & 1 & 0 & 0 & 0 & 0 & 0 & 0 \\ & e_5 & 0 & 0 & 0 & 0 & 0 & 0 & 0 & 0 & 0 & 1 & 0 & 0 & 0 & 0 & 0 \\ & f_0 & 0 & 0 & 0 & 0 & 0 & 0 & 0 & 0 & 0 & 0 & 1 & 0 & 0 & 0 & 0 \\ & f_1 & 1 & 0 & 0 & 0 & 0 & 0 & 0 & 0 & 1 & 0 & 0 & 0 & 1 & 0 & 0 \\ & f_2 & 0 & 0 & 0 & 0 & 0 & 0 & 0 & 0 & 0 & 0 & 0 & 0 & 0 & 1 & 0 \\ & f_3 & 0 & 0 & 0 & 0 & 0 & 0 & 0 & 0 & 0 & 0 & 0 & 0 & 0 & 0 & 1 \end{bmatrix}$															
Topological representation post – reflection															
$A_c = \begin{bmatrix} 5 & 1 & 11 & 6 & 16 & 4 & 26 & 39 & \dots & 31 & 23 \\ 5 & 2 & 11 & 8 & 17 & 1 & 26 & 40 & \dots & 31 & 26 \\ 6 & 1 & 11 & 13 & 17 & 37 & 27 & 37 & \dots & 31 & 26 \\ 7 & 2 & 11 & 13 & 17 & 37 & 27 & 37 & \dots & 31 & 27 \\ 6 & 3 & 11 & 16 & 18 & 2 & 28 & 38 & \dots & 31 & 34 \\ 6 & 3 & 11 & 21 & 18 & 38 & 27 & 39 & \dots & 31 & 36 \\ 7 & 4 & 11 & 21 & 18 & 38 & 27 & 39 & \dots & 32 & 22 \\ 8 & 3 & 11 & 23 & 19 & 1 & 28 & 40 & \dots & 32 & 24 \\ 8 & 4 & 12 & 7 & 19 & 37 & 29 & 17 & \dots & 32 & 26 \\ 9 & 5 & 12 & 8 & 20 & 2 & 29 & 19 & \dots & 32 & 28 \\ 9 & 6 & 12 & 14 & 20 & 38 & 29 & 25 & \dots & 32 & 35 \\ 9 & 13 & 12 & 16 & 21 & 3 & 29 & 27 & \dots & 32 & 36 \\ 9 & 15 & 12 & 22 & 21 & 39 & 29 & 33 & \dots & 32 & 38 \\ 9 & 17 & 12 & 24 & 22 & 4 & 29 & 34 & \dots & 33 & 37 \\ 9 & 19 & 13 & 1 & 22 & 40 & 30 & 18 & \dots & 33 & 38 \\ 10 & 5 & 14 & 2 & 23 & 3 & 30 & 20 & \dots & 34 & 37 \\ 10 & 7 & 13 & 3 & 23 & 39 & 30 & 25 & \dots & 35 & 38 \\ 10 & 14 & 14 & 4 & 24 & 4 & 30 & 28 & \dots & 34 & 39 \\ 10 & 15 & 15 & 1 & 24 & 40 & 30 & 33 & \dots & 35 & 40 \\ 10 & 18 & 15 & 2 & 25 & 37 & 30 & 35 & \dots & 36 & 39 \\ 10 & 20 & 16 & 3 & 25 & 38 & 31 & 21 & \dots & 36 & 40 \end{bmatrix}$															

#### 1.1 Graph Representation

Graph representation is extremely powerful in machine learning because it naturally encapsulates relationships and interdependencies among data entities, allowing algorithms to efficiently process complex networks and structures. This representation is particularly favorable because it enables the capture of non-linear patterns that traditional tabular data might miss, thus enhancing learning accuracy and predictive capabilities in diverse applications [1,2]. The data can be represented in a simple graph representation that integrates both the continuous variables (weights) within a vector  $x$ , and the discrete variables (sharing nodes) as a connectivity matrix  $C \in \{0,1\}^{n \times n}$ , where  $n$  represents the number of nodes in each SGO. We have shown a single sample from each symmetry from the main paper; the same method can be implemented for all other data. "Sharing nodes" in all the files means that the mentioned nodes are connected in a consecutive manner; for example, "e1, v4, e8" means  $e_1$  is connected with  $v_4$ , and  $v_4$  is connected with  $e_8$ .

### 1.1.1 Cubic – Samples

Cubic configurations are defined by nine planes of symmetry, resulting in 48 symmetric geometric objects (SGOs). Each SGO is structured with four vertex nodes ( $v_0$ ,  $v_1$ ,  $v_2$ , and  $v_3$ ), six edge nodes ( $e_0$ ,  $e_1$ ,  $e_2$ ,  $e_3$ ,  $e_4$ , and  $e_5$ ), and four face nodes ( $f_0$ ,  $f_1$ ,  $f_2$ , and  $f_3$ ). Following the methodology outlined in this study, we have successfully generated 800 cubic samples, the details of which are accessible via the previously mentioned link. Supp. Table 1 systematically presents the representation of a cubic sample, elucidating the structured layout and symmetrical attributes inherent within these samples.

### 1.1.2 Hexagonal – Samples

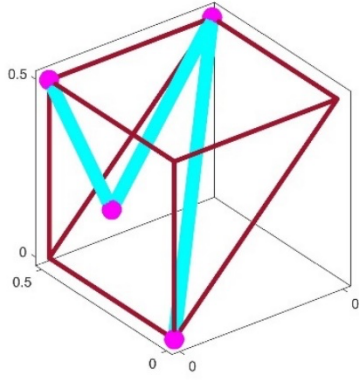
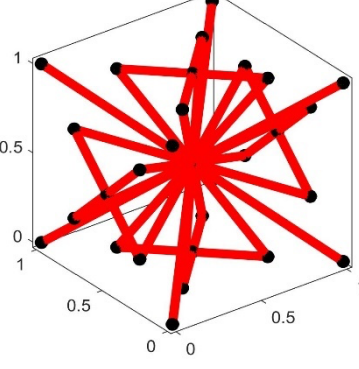
Hexagonal configurations are defined by seven planes of symmetry, resulting in 24 SGOS. Each SGO is structured with six vertex nodes ( $v_0, v_1, v_2, v_3, v_4$ , and  $v_5$ ), nine edge nodes ( $e_0, e_1, e_2, e_3, e_4, e_5, e_6, e_7$ , and  $e_8$ ), and five face nodes ( $f_0, f_1, f_2, f_3$ , and  $f_4$ ). Following the methodology outlined in this study, we have successfully generated 2500 hexagonal samples. Details of each sample can be found through the link provided earlier. Supp Table 2 clearly shows how a hexagonal sample can be represented in graph representation, highlighting its organized structure and symmetry.

Supp. Table 2. Graph representation of a hexagonal sample.

### 1.1.3 Tetragonal – Samples

Tetragonal configurations are defined by five planes of symmetry, resulting in 16 SGOs. Each SGO is structured with six vertex nodes ( $v_0, v_1, v_2, v_3, v_4$ , and  $v_5$ ), nine edge nodes ( $e_0, e_1, e_2, e_3, e_4, e_5, e_6, e_7$ , and  $e_8$ ), and five face nodes ( $f_0, f_1, f_2, f_3$ , and  $f_4$ ). Following the methodology outlined in this study, we have successfully generated 2500 tetragonal samples. Details of each sample can be found through the link provided earlier. Supp. Table 3 clearly shows a possible representation of the tetragonal sample.

Supp. Table 3. Graph representation of a tetragonal sample.

Data representation in the file																	
0.276637 0.250701 0.250701 0.000000 0.000000 -0.000000 0.925910 0.215266 -0.000000 -0.000000 -0.000000 0.925910 -0.000000 -0.000000 -0.000000 0.262989	0.000000 0.000000 0.265417 0.000000 0.262989 0.500000 0.500000 0.500000 0.500000 0.500000 0.500000 0.500000 0.500000 0.500000 0.000000	0.500000 0.500000 0.000000 0.500000 0.333333 0.333333 0.333333 0.333333 0.333333 0.000000 0.500000 0.500000 v0 v5 f0 v2															
Effective Elastic Properties (Stiffness Components)																	
0.276637 0.250701 0.250701 0.000000 0.000000 -0.000000 0.925910 0.215266 -0.000000 -0.000000 -0.000000 0.925910 -0.000000 -0.000000 -0.000000 0.262989	0.000000 0.000000 0.265417 0.000000 0.262989																
Topological representation pre – reflection																	
$x = \begin{bmatrix} 0.500 \\ 0.500 \\ 0.500 \\ 0.500 \\ 0.500 \\ 0.500 \\ 0.500 \\ 0.500 \\ 0.500 \\ 0.500 \\ 0.500 \\ 0.500 \\ 0.500 \\ 0.500 \\ 0.500 \\ 0.500 \\ 0.500 \end{bmatrix}$	$C = \begin{bmatrix} - & v_0 & v_1 & v_2 & v_3 & v_4 & v_5 & e_0 & e_1 & e_2 & e_3 & e_4 & e_5 & e_6 & e_7 & e_8 & f_0 & f_1 & f_2 & f_3 & f_4 \\ v_0 & 1 & 0 & 0 & 0 & 1 & 0 & 0 & 0 & 0 & 0 & 0 & 0 & 0 & 0 & 0 & 0 & 0 & 0 & 0 & 0 \\ v_1 & 0 & 1 & 0 & 0 & 0 & 0 & 0 & 0 & 0 & 0 & 0 & 0 & 0 & 0 & 0 & 0 & 0 & 0 & 0 & 0 \\ v_2 & 0 & 0 & 1 & 0 & 0 & 0 & 0 & 0 & 0 & 0 & 0 & 0 & 0 & 0 & 0 & 0 & 0 & 1 & 0 & 0 \\ v_3 & 0 & 0 & 0 & 1 & 0 & 0 & 0 & 0 & 0 & 0 & 0 & 0 & 0 & 0 & 0 & 0 & 0 & 0 & 0 & 0 \\ v_4 & 0 & 0 & 0 & 0 & 1 & 0 & 0 & 0 & 0 & 0 & 0 & 0 & 0 & 0 & 0 & 0 & 0 & 0 & 0 & 0 \\ v_5 & 1 & 0 & 0 & 0 & 0 & 1 & 0 & 0 & 0 & 0 & 0 & 0 & 0 & 0 & 0 & 0 & 0 & 1 & 0 & 0 \\ e_0 & 0 & 0 & 0 & 0 & 0 & 1 & 0 & 0 & 0 & 0 & 0 & 0 & 0 & 0 & 0 & 0 & 0 & 0 & 0 & 0 \\ e_1 & 0 & 0 & 0 & 0 & 0 & 0 & 1 & 0 & 0 & 0 & 0 & 0 & 0 & 0 & 0 & 0 & 0 & 0 & 0 & 0 \\ e_2 & 0 & 0 & 0 & 0 & 0 & 0 & 0 & 1 & 0 & 0 & 0 & 0 & 0 & 0 & 0 & 0 & 0 & 0 & 0 & 0 \\ e_3 & 0 & 0 & 0 & 0 & 0 & 0 & 0 & 0 & 1 & 0 & 0 & 0 & 0 & 0 & 0 & 0 & 0 & 0 & 0 & 0 \\ e_4 & 0 & 0 & 0 & 0 & 0 & 0 & 0 & 0 & 0 & 1 & 0 & 0 & 0 & 0 & 0 & 0 & 0 & 0 & 0 & 0 \\ e_5 & 0 & 0 & 0 & 0 & 0 & 0 & 0 & 0 & 0 & 0 & 1 & 0 & 0 & 0 & 0 & 0 & 0 & 0 & 0 & 0 \\ e_6 & 0 & 0 & 0 & 0 & 0 & 0 & 0 & 0 & 0 & 0 & 0 & 1 & 0 & 0 & 0 & 0 & 0 & 0 & 0 & 0 \\ e_7 & 0 & 0 & 0 & 0 & 0 & 0 & 0 & 0 & 0 & 0 & 0 & 0 & 1 & 0 & 0 & 0 & 0 & 0 & 0 & 0 \\ e_8 & 0 & 0 & 0 & 0 & 0 & 0 & 0 & 0 & 0 & 0 & 0 & 0 & 0 & 1 & 0 & 0 & 0 & 0 & 0 & 0 \\ f_0 & 0 & 0 & 1 & 0 & 0 & 1 & 0 & 0 & 0 & 0 & 0 & 0 & 0 & 0 & 0 & 0 & 0 & 1 & 0 & 0 \\ f_1 & 0 & 0 & 0 & 0 & 0 & 0 & 0 & 0 & 0 & 0 & 0 & 0 & 0 & 0 & 0 & 0 & 0 & 0 & 1 & 0 \\ f_2 & 0 & 0 & 0 & 0 & 0 & 0 & 0 & 0 & 0 & 0 & 0 & 0 & 0 & 0 & 0 & 0 & 0 & 0 & 0 & 1 \\ f_3 & 0 \\ f_4 & 0 & 0 & 0 & 0 & 0 & 0 & 0 & 0 & 0 & 0 & 0 & 0 & 0 & 0 & 0 & 0 & 0 & 0 & 0 & 1 \end{bmatrix}$																
Topological representation post – reflection																	
$X = \begin{bmatrix} 0.000 & 0.000 & 0.000 \\ 0.000 & 0.000 & 1.000 \\ 0.000 & 0.250 & 0.250 \\ 0.000 & 0.250 & 0.750 \\ 0.000 & 0.500 & 0.500 \\ 0.000 & 0.750 & 0.250 \\ 0.000 & 0.750 & 0.750 \\ 0.000 & 1.000 & 0.000 \\ 0.000 & 1.000 & 1.000 \\ 0.250 & 0.250 & 0.000 \\ 0.250 & 0.250 & 1.000 \\ 0.250 & 0.500 & 0.500 \\ 0.250 & 0.750 & 0.000 \\ 0.250 & 0.750 & 1.000 \\ 0.500 & 0.500 & 0.000 \\ 0.500 & 0.500 & 1.000 \\ \dots & \dots & \dots \end{bmatrix}$	$A_C = \begin{bmatrix} 3 & 15 & \dots & \dots \\ 4 & 15 & 15 & 21 \\ 5 & 3 & 15 & 22 \\ 5 & 4 & 15 & 28 \\ 5 & 6 & 15 & 29 \\ 5 & 7 & 16 & 11 \\ 6 & 15 & 16 & 13 \\ 7 & 15 & 16 & 18 \\ 10 & 15 & 16 & 20 \\ 11 & 15 & 17 & 15 \\ 12 & 15 & 18 & 15 \\ 13 & 15 & 19 & 15 \\ 14 & 10 & 20 & 15 \\ 14 & 12 & 23 & 15 \\ 14 & 17 & 24 & 15 \\ 14 & 19 & 25 & 23 \\ 15 & 1 & 25 & 24 \\ 15 & 2 & 25 & 26 \\ 15 & 8 & 25 & 27 \\ 15 & 9 & 26 & 15 \\ \dots & \dots & 27 & 15 \end{bmatrix}$																

### 1.1.4 Orthotropic Samples

Orthotropic configurations are defined by three planes of symmetry, resulting in 8 SGOs. Each SGO is structured with eight vertex nodes ( $v_0, v_1, v_2, v_3, v_4, v_5, v_6$ , and  $v_7$ ), twelve edge nodes ( $e_0, e_1, e_2, e_3, e_4, e_5, e_6, e_7, e_8, e_9, e_{10}$ , and  $e_{11}$ ), and six face nodes ( $f_0, f_1, f_2, f_3, f_4$ , and  $f_5$ ). Following the methodology outlined in this study, we have successfully generated 2500 orthotropic samples. Details of each sample can be found through the link provided earlier. Supp. Table 4 clearly shows a possible representation of an orthotropic sample.

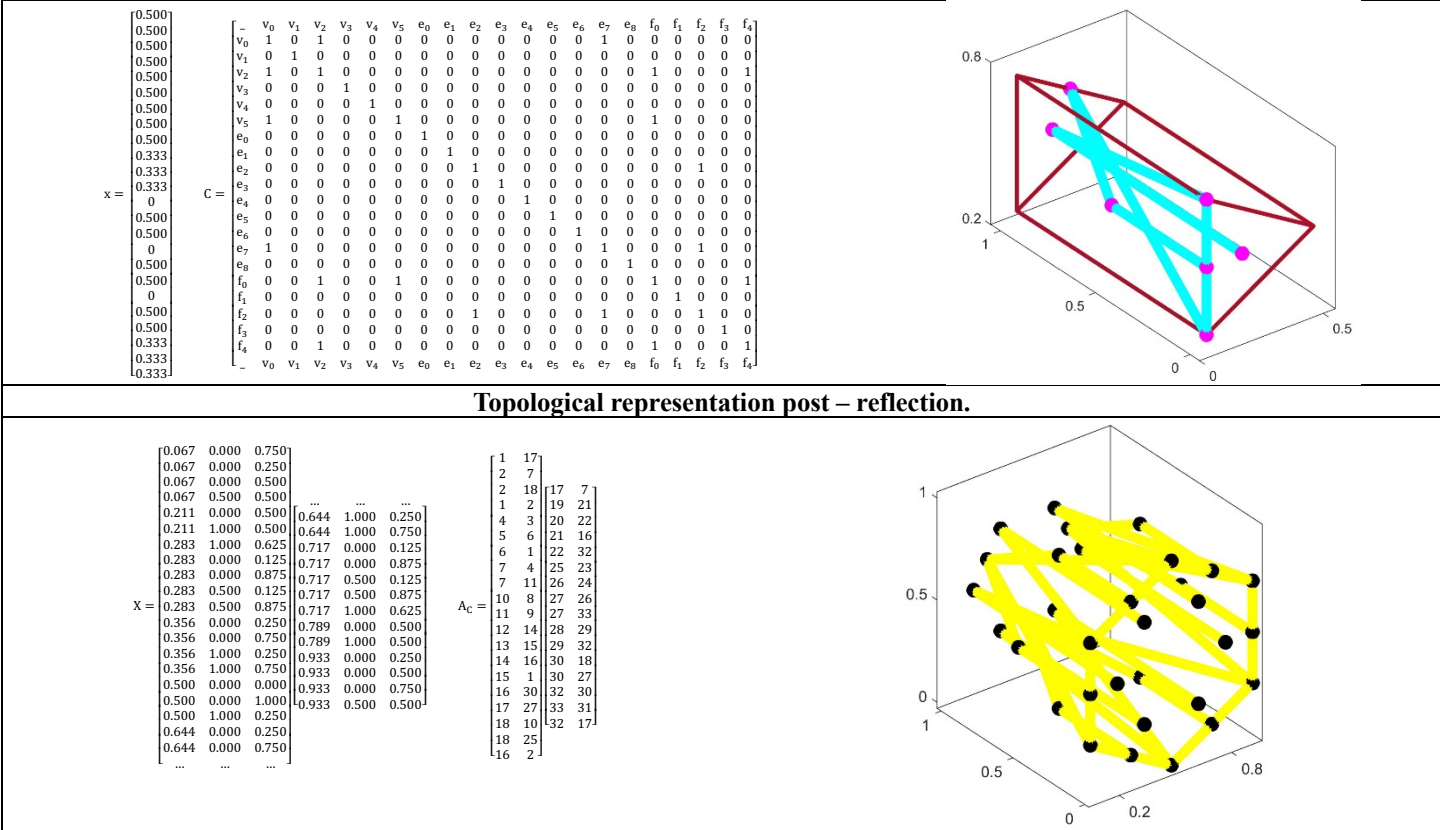
### 1.1.5 Trigonal Samples

Trigonal configurations are defined by three planes of symmetry, resulting in 3 SGOs. Each SGO is structured with six vertex nodes ( $v_0, v_1, v_2, v_3, v_4$ , and  $v_5$ ), nine edge nodes ( $e_0, e_1, e_2, e_3, e_4, e_5, e_6, e_7$ , and  $e_8$ ), and five face nodes ( $f_0, f_1, f_2, f_3$ , and  $f_4$ ). Following the methodology outlined in this study, we have successfully generated 2500 trigonal samples. Details of each sample can be found through the link provided earlier. Supp. Table 5 clearly shows a possible representation of the trigonal sample.

Supp. Table 4. Graph representation of an orthotropic sample.

Supp. Table 5. Graph representation of a trigonal sample.

Data representation in the file	
2.462981	0.001870 0.001522 0.000000 0.000000 0.001062 0.181224 0.118877 0.000000 0.000000 -0.001314 0.085674 0.000000 0.000000 0.000752 0.005542 -0.001817 0.000000 0.005855 -0.000000 0.006859 0.500000 0.500000 0.500000 0.500000 0.500000 0.500000 0.500000 0.500000 0.333333 0.333333 0.333333 0.333333 0.000000 0.500000 0.500000 0.000000 0.500000 0.500000 0.000000 0.500000 0.333333 0.333333 0.333333 e2 f2 e7 v0 v2 f4 fo
Effective Elastic Properties (Stiffness Components)	
0.939066	0.018836 0.801839 0.000000 -0.000000 -0.000000 0.014054 0.003813 -0.000000 -0.000000 0.000000 0.808083 -0.000000 -0.000000 -0.000000 0.006736 -0.000000 -0.000000 0.006924 -0.000000 0.759607



### 1.1.6 Monoclinic Samples

Monoclinic configurations are defined by a single plane of symmetry, resulting in 2 SGOS. Each SGO is structured with eight vertex nodes ( $v_0, v_1, v_2, v_3, v_4, v_5, v_6$ , and  $v_7$ ), twelve edge nodes ( $e_0, e_1, e_2, e_3, e_4, e_5, e_6, e_7, e_8, e_9, e_{10}, e_{11}$ ), and six face nodes ( $f_0, f_1, f_2, f_3, f_4$ , and  $f_5$ ). Following the methodology outlined in this study, we have successfully generated 2500 Monoclinic samples. Details of each sample can be found through the link provided earlier. Supp. Table 6 clearly shows a possible representation of a Monoclinic sample.

### 1.2 Parametric Representation

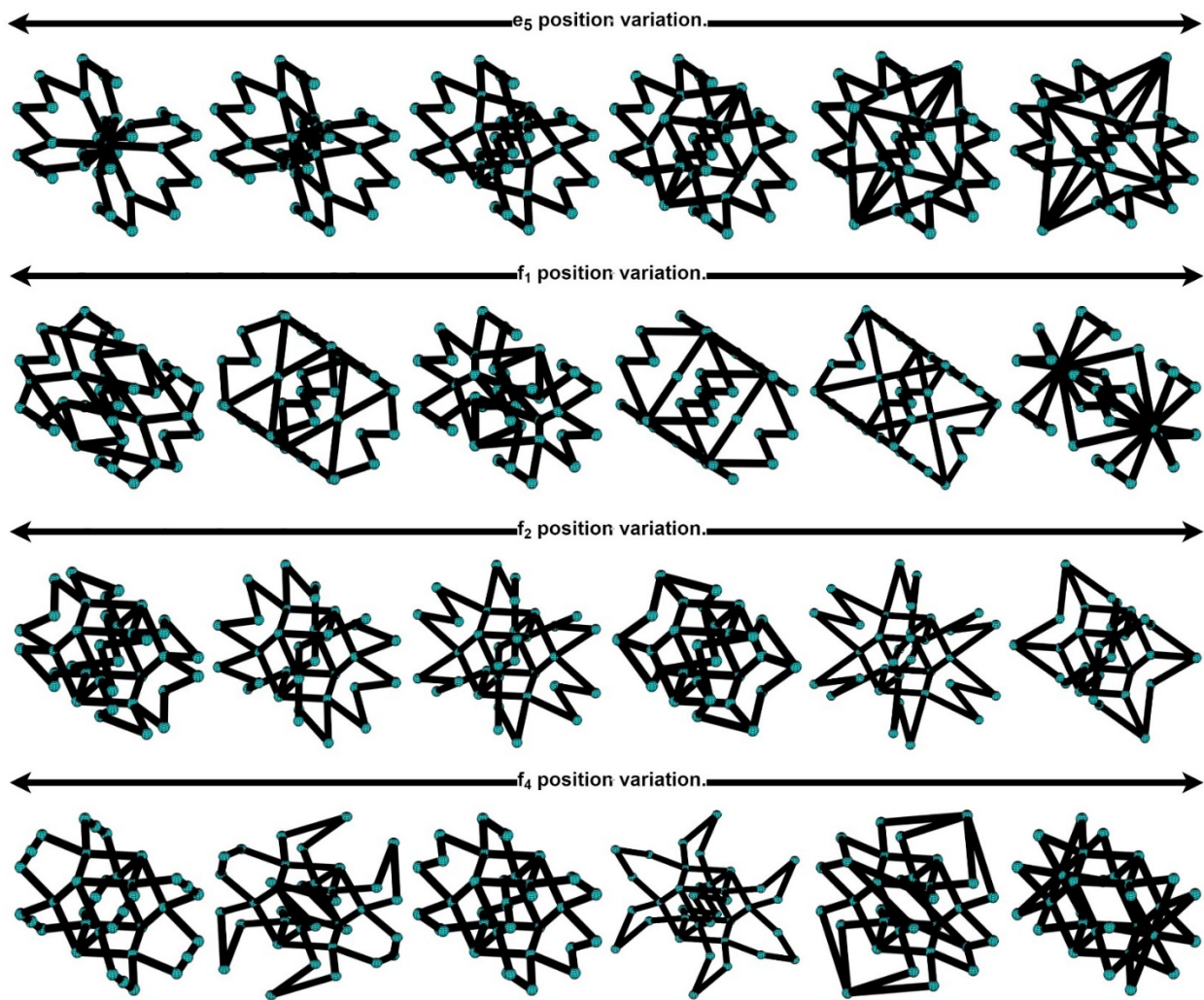
Additionally, the data can be represented using a parametric representation, which benefits from the tiltability of the approach. This means that a single unit-cell can be represented as a representative unit-cell; by altering the weights, a vast dataset can be generated. In this supplementary material, we have showcased a single representative tetragonal unit-cell, established from the following shared nodes:  $e_5, f_1, f_2$ , and  $f_4$ . This mentioned unit-cell can be represented using 10 continuous variables:  $w_5, w_{11}, w_{12}, w_{13}, w_{21}, w_{22}, w_{23}, w_{41}, w_{42}$ , and  $w_{43}$ . We have established the elastic stiffness parameters of 2,500 samples through the numerical homogenization discussed in the main paper. The numerical simulation used a base material with a Young's modulus ( $E_s$ ) of 200 GPa, a Poisson's ratio ( $\nu$ ) of 0.3, and a truss diameter of 0.025 meters. The samples are available via the same link mentioned the name "parametric samples - e5f1f2f4.csv". Supp Table 7 displays a sample represented in parametric representation, which can be directly utilized in machine learning predictions.

In addition, Supp Fig. 1. illustrates some of the configurations that result from the variation in the positions of the four shared nodes of the representative sample. Supp Fig. 2. demonstrates that a single representative unit-cell with a fixed truss diameter can result in an acceptable range of mechanical properties based solely on the chosen samples. This range could be expanded further by varying the truss diameter and exploring more extensively rather than just sampling. In addition to that, a potential approach to achieving a diverse dataset with parametric representation is by including more representative unit-cells within a single dataset. Each representative unit-cell would be assigned a number that could be used as a discrete variable, similar to the approach used in [3], where they utilized seven representative parameters to establish their dataset.

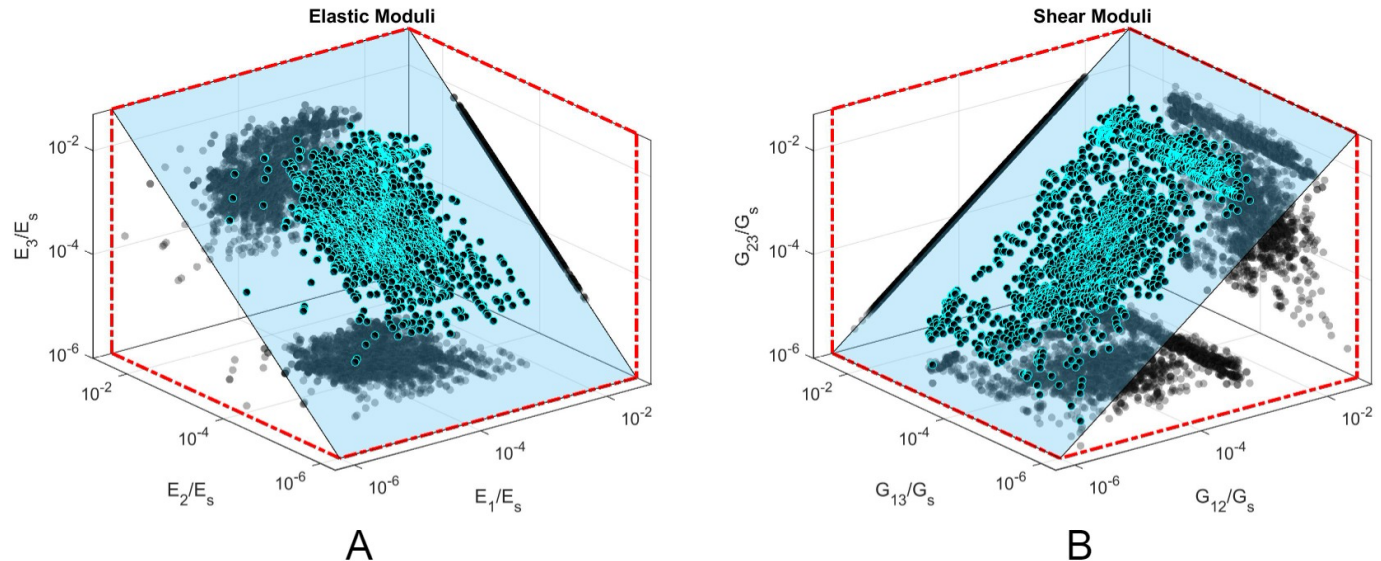
Supp. Table 6. Graph representation of a Monoclinic sample.

Supp. Table 7. Parametric representation of a tetragonal unit-cell constructed from the sharing nodes e<sub>5</sub> f<sub>1</sub> f<sub>2</sub> f<sub>4</sub>.

Data representation in the file
0.192447 0.159778 0.159778 -0.000000 -0.000000 0.000000 0.347428 0.004558 -0.000000 -0.000000 0.000000 0.347428 -0.000000 0.000000 -0.000000 0.045306 -0.000000 0.000000 0.004529 -0.000000 0.045306 0.000000 0.333333 0.666667 0.000000 0.333333 0.333333 0.333333 0.000000 0.000000 1.000000
Effective Elastic Properties (Stiffness Components)
0.192447 0.159778 0.159778 -0.000000 -0.000000 0.000000 0.347428 0.004558 -0.000000 -0.000000 0.000000 0.347428 -0.000000 0.000000 -0.000000 0.045306 -0.000000 0.000000 0.004529 -0.000000 0.045306
Topological representation
0.000000 0.333333 0.666667 0.000000 0.333333 0.333333 0.333333 0.000000 0.000000 1.000000



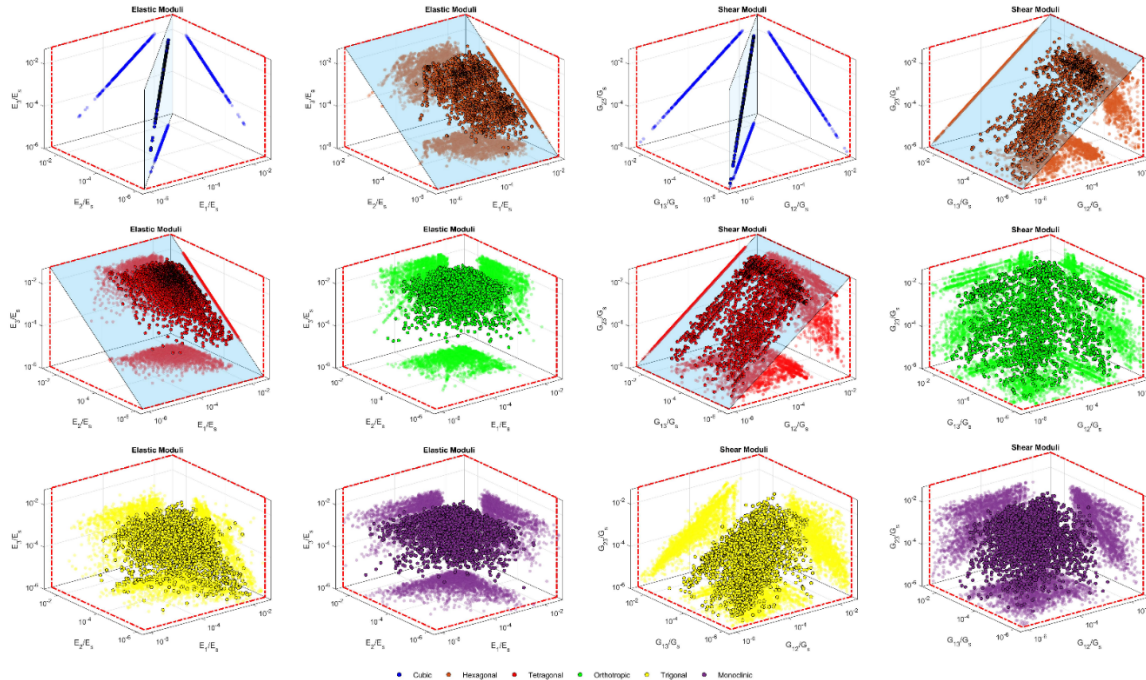
Supp Fig. 1. Tetragonal topologies are generated through the variation of the weights of topology, constructed from the shared nodes  $e_5$ ,  $f_1$ ,  $f_2$ , and  $f_4$ .



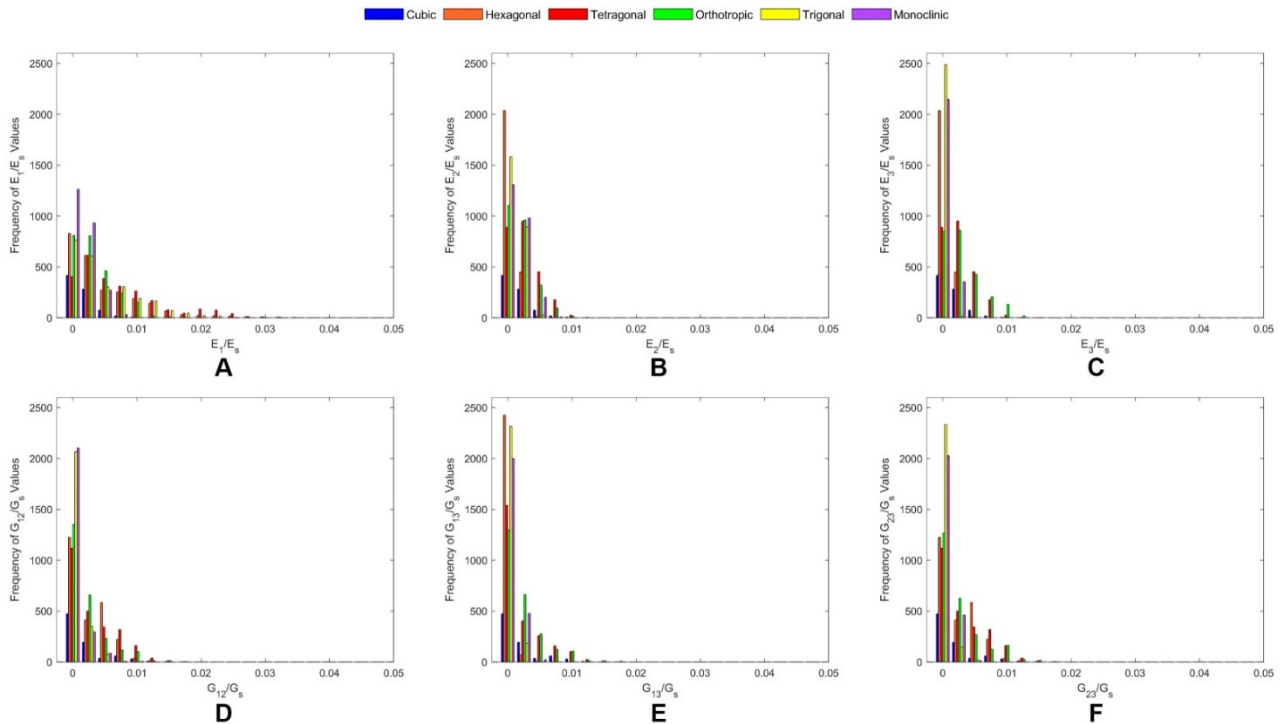
Supp Fig. 2. Relative effective elastic properties of the samples chosen from the representative tetragonal unit-cell  $e_5$ ,  $f_1$ ,  $f_2$ ,  $f_4$ : A. Relative effective Young's moduli in the three directional primary axes, and B. Relative effective shear moduli in the three directional primary axes.

## 2. Samples Statistical Data

In this section of the supplementary material, we provide additional results that support Section 4. In Supplementary Figure 3, we have included a distinct property space for each symmetry type to facilitate clear visualization. Furthermore, Supplementary Figure 4 illustrates the relative effective directional elastic properties using statistical parameters, which enhances the discussion in the main paper by demonstrating the influence of each symmetry on the elastic properties.



Supp Fig. 3. Relative effective Young's moduli and effective shear moduli of all the symmetry methods for the sampled data.



Supp Fig. 4. Histograms of the directional elastic properties for samples generated using different symmetry methods, displaying values for: A.  $E_1/E_s$ , B.  $E_2/E_s$ , C.  $E_3/E_s$ , D.  $G_{12}/G_s$ , E.  $G_{13}/G_s$ , and F.  $G_{23}/G_s$ .

### **3. Reference.**

- [1] Ju W, Fang Z, Gu Y, et al. A Comprehensive Survey on Deep Graph Representation Learning. *Neural Networks* 2024; 173: 106207. doi:<https://doi.org/10.1016/j.neunet.2024.106207>
- [2] Khoshrafter S, An A. A Survey on Graph Representation Learning Methods. *ACM Trans Intell Syst Technol* 2024; 15. doi:10.1145/3633518
- [3] Bastek J-H, Kumar S, Telgen B, et al. Inverting the structure–property map of truss metamaterials by deep learning. *Proceedings of the National Academy of Sciences* 2022; 119: e2111505119. doi:10.1073/pnas.2111505119